2013 IREP Symposium-Bulk Power System Dynamics and Control -IX (IREP), August 25-30, 2013, Rethymnon, Greece

A Battery Energy Storage Based Virtual Synchronous Generator

A. Vassilakis,
P. Kotsampopoulos, N. Hatziargyriou
National Technical University of Athens.
e-mail: avassil@mail.ntua.gr, kotsa@power.ece.ntua.gr,
nh@power.ece.ntua.gr

V. Karapanos
IEEE menber
e-mail: vkarapanos@gmail.com

Abstract

The purpose of this paper is to investigate the interaction of the Virtual Synchronous Generator (VSG) units with the grid. Within this scope, test-scenarios of different power systems with increasing VSG penetration levels, are simulated and evaluated. The ability of a battery storage system to provide primary frequency regulation, as part of a virtual synchronous generator, is also examined whereas several control strategies are used to properly manage the battery storage system according to the technical specifications of the ENTSO-E.

Introduction

Nowadays interest in generating electricity using relatively small scale decentralized generators is increasing. These small power generators are connected mainly at distribution level influencing the technical aspects of the distribution grid [1]. The traditional power system is characterized by a relatively small number of large centralized power plants, based on synchronous generators, in order to accomplish the power balance between energy production and energy demand. Up to now, the short-term dynamic stability of the power system has been mainly based on the intrinsic rotor inertia of synchronous generators (SG). As the classic “vertical” power system transforms into a more “horizontal” power system with a greater penetration of inverter coupled generating facilities, this “naturally” provided inertia will gradually be reduced. The frequency of a power system with low inertia will change rapidly for abrupt variations in generation or load. In this case, additional frequency response ancillary services must be provided to ensure that frequency limits are not exceeded [2].

The provision of Virtual rotational inertia in order to reinforce the stability of the power system, has been introduced to the grid-connected system as a promising solution. The idea of operating an inverter to mimic a synchronous generator has been gaining popularity in the recent years. Several techniques have been proposed towards this direction. The Virtual Synchronous Machine (VISMA) performs real time calculations of electromagnetic synchronous machine properties [3]. The voltages at the point of common coupling with the grid are measured to calculate the phase currents of the VISMA. These currents are used as reference for a current-controlled inverter. Another similar concept is that of synchonverter, where the phase current is measured and the output voltage is real time calculated so that it is equal to the back EMF that a synchronous generator would produce under the same conditions on the grid [4]. The Virtual Synchronous Generator (VSG) models the rotational inertia of a synchronous machine without considering other synchronous machine properties [5].

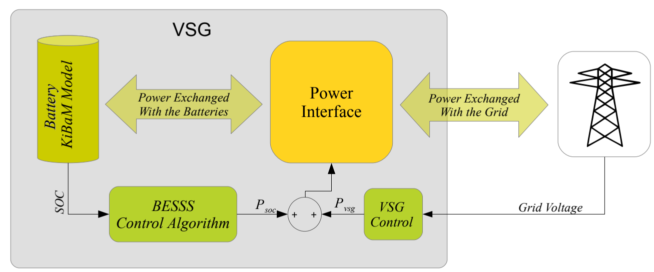

Fig. 1. The principle of Battery Energy Storage Based Virtual Synchronous Generator.

The general concept of a VSG unit is presented in Fig. 1. A Battery Energy Storage System (BESS) exchanges power with the grid according to BESS and VSG control algorithms. The outline of the battery based VSG model used in this study is given in the following section. The VSG performance is afterward studied, through various test-scenarios when the VSG penetration level increases. The last part investigates the ability of the battery based VSG to provide primary frequency regulation. Real frequency data are used to test and compare the performance of several battery management strategies.

VSG Model Implementation

High level control

The main objective of the control of a VSG is to emulate the two inherent features of a synchronous generator that are identified to be crucial in the stable and reliable operation of a power system. These features are the rotational inertia due to the rotating masses and the speed-droop characteristics of a synchronous generator for load sharing.

The differential equation that describes the rotor acceleration

978-1-4799-0199-9/13/ $31.00 ©2013 IEEE

of a synchronous machine given the inertia constant J is:

$$P_m - P_e = \frac{d(1/2 J\omega^2)}{dt} \tag{1}$$

where, P_m is the mechanical power of the generator and P_e is the electrical power of the generator, while ω is the angular velocity of the rotor.

The rate of change of speed of the rotor is dependent on the moment of inertia of the rotating mass. The kinetic energy that is stored during the steady operation of the generator is very beneficial at an imbalance of torques. This kinetic energy will be absorbed by the system to mitigate the speed deviations from the synchronous speed [6].

By substituting $P_m - P_e$ with P_{VSG} in eq. (1) an expression for the emulation of rotational inertia is given by eq. (2)

$$P_{VSG} = K_d \frac{d\omega}{dt} \tag{2}$$

In power generation, rotor speed regulation is achieved with the use of a governor. Hence, to maintain constant frequency under normal operating conditions, an auxiliary control is required which responds to slow frequency deviations. For this reason a droop part is added to eq. (2) as follows:

$$P_{VSG} = K_d \frac{d\omega}{dt} + K_p(\omega - \omega_{ref}) \tag{3}$$

According to eq. (3), a VSG exchanges power with the grid in case the frequency deviates from the nominal value and/or a rate of change of frequency is detected. The K_d coefficient is a constant that defines the amount of active power interchanged with the network when the maximum specified rate of change of frequency (Hz/s) occurs. The K_p is the droop coefficient and defines the power that needs to be absorbed or injected into the system due to the deviation of frequency from the reference value [7].

The control law of eq. (3) is depicted in Fig. 2 in a block diagram form. The controller contains a derivative term that may produce abrupt reference signal leading the system over its operation limits. Therefore, it is good practice to filter the frequency in order to calculate the active power reference of the VSG.

Low level control

The purpose of the low level control is to calculate the output current. Fig. 3 shows the most important parts of the three phase VSG control unit. The first block performs the transformation of the *abc*-phase voltages at the point of common coupling to the synchronous reference. The parameter

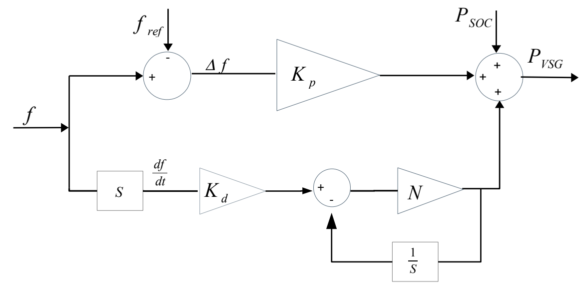

Fig. 2. Block diagram of the high level control of the VSG.

θ is extracted by a Phase Locked Loop (PLL) block and defines the reference frame of the transformation. The second block, which refers to the high level control, calculates the active and reactive power that should be produced by the VSG, taking as input the frequency of the system and the phase voltage at the *dq* reference frame. Within the scope of this work only the active power is taken into consideration setting the reactive power equal to zero ($K_V = 0$ in Fig. 3). The phase voltage along with the active power, are passed to the current reference calculation block which determines the instantaneous current references.

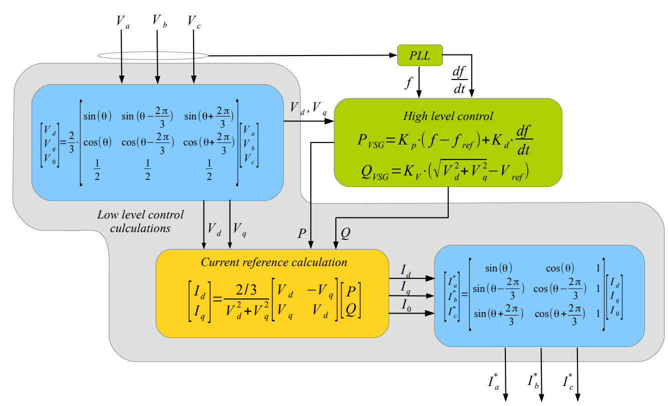

Fig. 3. Configuration of a VSG unit consisting of a High and Low level control.

The model of the VSG's power circuit, consists of a three phase controlled current source. As long as no switching devices are included, the "average model" of the VSG is based on the energy conservation principle, which means that the instantaneous power on the AC side must be the same with the DC side (assuming ideal conversion). The DC current can be therefore computed as:

$$P_{DC} = P_{AC} \Longleftrightarrow I_{DC} = \frac{v_a i_a + v_b i_b + v_c i_c}{V_{DC}} \tag{4}$$

Battery modeling

The battery energy storage system is implemented according to the Kinetic Battery Model (KiBaM) [8]. This model is divided into two parts as shown in Fig. 4:

- The capacity model, which estimates the state of charge (SOC) of batteries.
- The voltage model, that calculates the terminal voltage of the batteries.

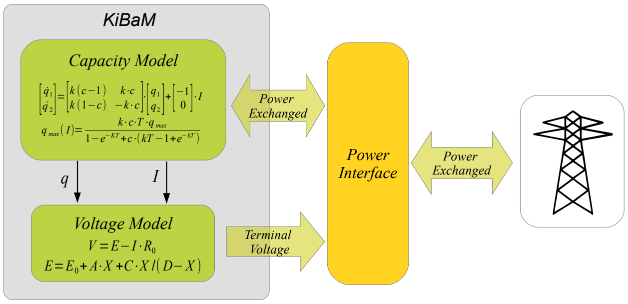

Fig. 4. The principle of Kinetic Battery Model.

The capacity model is able to address both the recovery and the rate capacity effect of the battery. The first one refers to the effect where an amount of charge becomes available to the battery when no charge current is presented, while the second one refers to the effect where less charge can be drawn from a battery when the discharge current is increased.

The voltage model of the second block considers the battery as a voltage source in series with a resistance that is assumed to be constant. The terminal voltage depends both on the state of charge as well as on the amount of the current drawn from the battery.

Operation and Results

The objective of this section is to prove that the VSG is capable to decrease the size of frequency deviations that are caused by load variations in different networks. In order to evaluate the contribution of the VSG in the overall stability of the system, its steady state operation is disturbed by changing the actual total load of the system. The disturbances are evaluated in respect to the penetration level of the VSG.

The penetration level can be calculated as a function of the nominal VSG active power generation over the total load demand [9].

$$\%VSG_{penetrationlevel} = \frac{\sum P_{VSG}}{\sum P_{Load}} \times 100\% \qquad (5)$$

Parallel operation of VSG and SG in a large network

The test network comprises of a generating station, a VSG and a variable load that are connected to the grid through a transmission line. A load changes its value according to a simple load profile, causing disturbances to the frequency of the system. The simulation network is shown in Fig. 5.

The power consumption on constant load is 90 kW while the load deviation does not exceed 20% of the nominal power of the generating station (112 kVA). The penetration of the VSG increases gradually. In this way three sub-scenarios are examined, with penetration levels of 0%, 10%, and 30%, respectively. Graph (b) Fig. 6 illustrates the frequency response of the power system due to the load changes while the penetration level of the VSG increases. The active power produced and absorbed by the VSG for each level of VSG penetration is depicted in Graph (c) of Fig. 6.

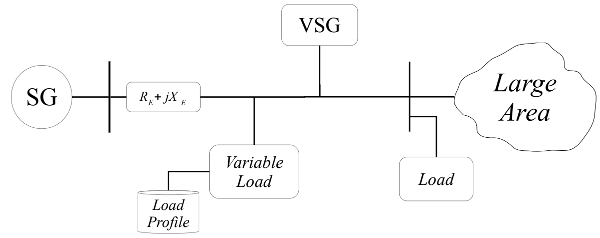

Fig. 5. One area system comprising a SG and a VSG connected to the grid.

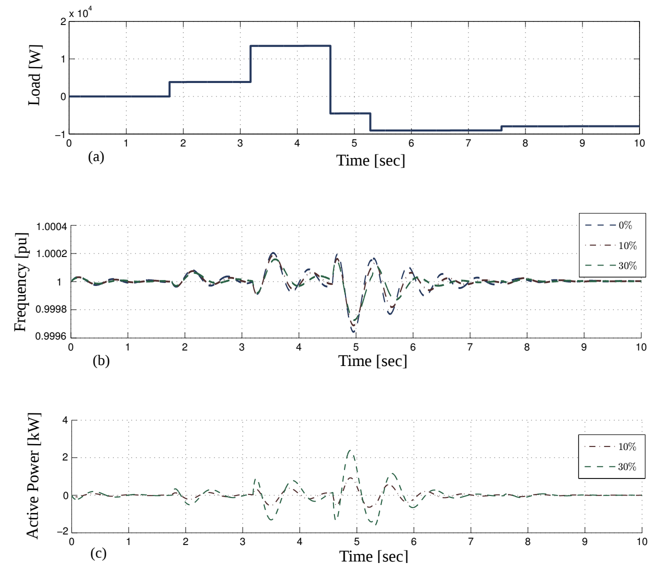

Fig. 6. Frequency and active power of the system during load variations. a) Load profile, b) Frequency responce, c) Active power response.

Simulation of the VSG in a two area system

In this scenario, the system of Fig. 7 consists of two generating stations delivering power through two typical H.V. transmission lines. The system comprises of constant and variable loads and a VSG unit. The penetration level of the VSG is rated at 10% while the power consumption on constant load is 300 MW. The generation stations have nominal power of 255 MVA and 1000 MVA respectively. The variable load follows the load profile of Fig. 8(a).

Fig. 8(b), illustrates the simulation results for the two modes of operation, with a 10% penetration of the VSG and without the VSG, the comparison of which makes discernible the effect of the VSG unit on the maximum frequency deviation.

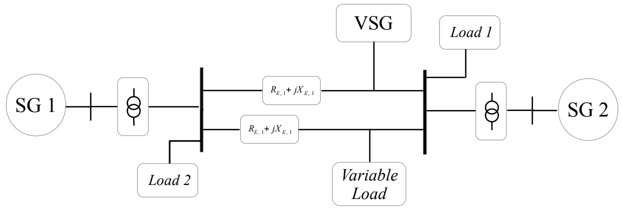

Fig. 7. Two area system comprising two SG's and VSG.

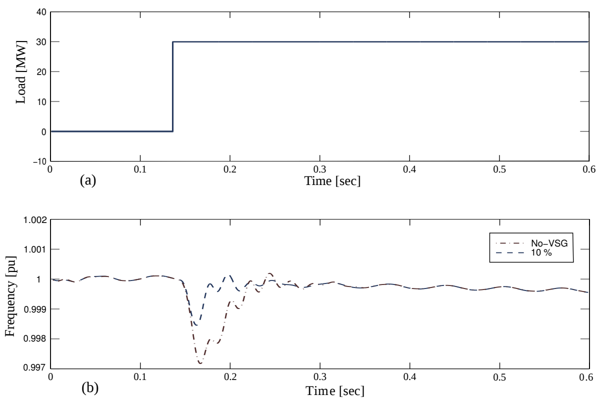

Fig. 8. Frequency response for two modes of operation: with 10% penetration of VSG and without VSG for the two area system.

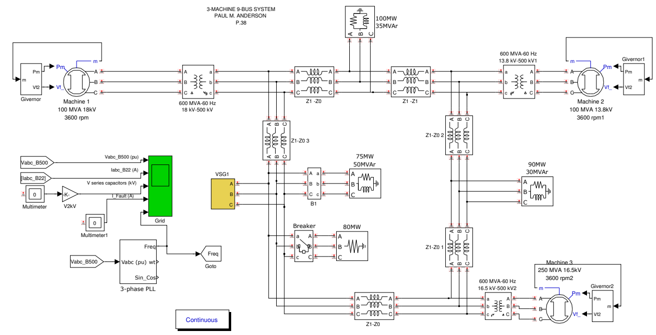

Fig. 9. Simulink model of the 3-machine 9-bus system.

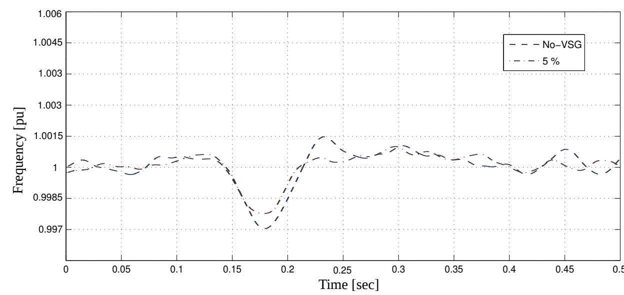

Fig. 10. Grid frequency variation for two modes of operation: with a 5% penetration of a VSG and without a VSG for the 9-bus simulation system.

Operation of VSG in a three area system

The simulation system is constituted by the classical nine bus dynamic power system that includes three generating stations and three loads [10]. This system is large enough to be nontrivial and thus permits the illustration of more realistic results. The complete block diagram of the system, is presented in Fig. 9.

The objective of the simulation is to obtain the response of the frequency after the transient is introduced. A load of 20% of the total power is connected, initiating the disturbance. The total active load of the system is $345\,\mathrm{MW}$ while the penetration level of the virtual synchronous generator is rated at $5\,\%$.

The dynamic response of the frequency of the power system for the two modes of operation, is shown in Fig. 10.

Battery management strategies

Frequency control according to ENTSO-E

A requirement for the operation of the power system is the balance between power supply and power demand at any time. Even under normal conditions, the demand of the system is subjected to continuous changes. Therefore, several levels of controls are performed to maintain the system frequency at its nominal value. Fig. 11, demonstrates the three types of control performed in different successive steps according to the technical specification of ENTSO-E [11]. The primary control aims at the operational reliability of the power system of the synchronous area and stabilizes the system frequency at a stationary value after a disturbance. In case of an incident with a large frequency drop, the activation of primary control reserve (activated within seconds lasting less than $15\,\mathrm{min}$) is followed up by a secondary control reserve (activated within minutes) which is supported and followed up by the tertiary control reserve.

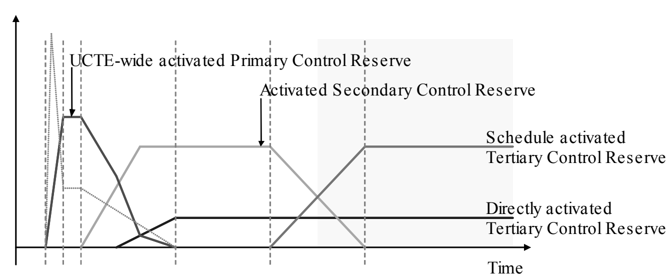

Fig. 11. Principle frequency deviation and subsequent activation of reserves [11].

The ENTSO-E rules specify that the nominal frequency should be $50\,\mathrm{Hz}$ and define a frequency zone of $\pm 20\,\mathrm{mHz}$ within which the frequency variations are considered non critical. The maximum of $\pm 200\,\mathrm{mHz}$ from nominal frequency is indicated as a permissible deviation where the full primary control has to be activated.

Battery based VSG for frequency regulation

In this section the effect of operating the VSG for primary frequency regulation on the battery energy storage system is investigated. The management of batteries imposes selective restrictions on the operation of VSG, e.g. when the battery is fully charged no more active power can be absorbed. Several battery management strategies have been assessed according to the minimum battery capacity required for the accomplishment of frequency regulation [12].

The current framework uses real frequency data for the time period 1st to 8th of July 2012 that were provided by the Greek independent power transmission operator (ADMIE). For simulation reasons we choose a hypothetical primary reserve contract of $P_n = 1\,\mathrm{MW}$ which states that the system is able to produce this power for at least $15\,\mathrm{min}$ in accordance to ENTSO-E. Consequently, the minimum acceptable energy of the storage system would be: $E_{reserve} = P_n \cdot {}^{h}/_{4}$.

The main function of the frequency control is to compensate the frequency deviations from the grid. The size and the rate of change of the deviation determine how much power should be exchanged with the network. When the frequency is changed to values that exceed the non critical window, the control should react by absorbing or injecting power according to eq. (3).

Conclusively, the primary reserve power P_n should be provided when the maximum allowed frequency deviation of $\pm 200\,\mathrm{mHz}$ occurs or when the maximum specified rate of change of frequency ($0.4\,{}^{\mathrm{Hz}}/_{\mathrm{s}}$) is realized.

Control strategies

Constant charge-discharge strategy: Since the VSG controls are designed to work bidirectionally, the nominal state of charge should be in the middle of the upper and lower operational boundaries of the storage system. If we determine the maximum depth of discharge up to $40\,\%$ of the total capacity of the storage, then the reference state of charge is $SOC_{ref} = 80\,\%$.

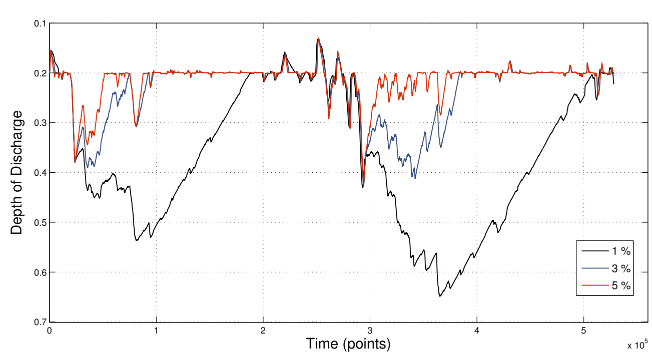

Fig. 12. Depth of discharge of the storage as a function of time for the constant recharge control with charge-discharge power of $1\,\%$, $3\,\%$, and $5\,\%$ of nominal power P_n.

A control strategy, is considered where the batteries are charging at non-critical periods ($|\Delta f| < 20\,mHz$) and a separate algorithm is taking to consideration the state of charge of the storage. The objective is - alongside with primary frequency regulation - to maintain the battery state of charge at the reference level, charging or discharging respectively, when the SOC is less or greater than the specified value SOC_{ref}. A small portion $1\,\%$ to $5\,\%$ of P_{nom} is used for charge-recharge power. The control algorithm can be formulated in the following equation:

$$P_{VSG} = \begin{cases} K_p \cdot (f - f_{ref}) + K_d \cdot \dfrac{df}{dt}, & |\Delta f| \geq 20\,\mathrm{mHz} \\ K_{soc} \cdot sgn(SOC - SOC_{ref}) & |\Delta f| < 20\,\mathrm{mHz} \end{cases} \tag{6}$$

where sgn is the sign function and K_{soc} denotes the charge-discharge power when the system is out of the critical window.

Fig. 12, illustrates the depth of discharge of the storage as a function of time for different modes of operation with charge-discharge power of $1\,\%$, $3\,\%$, and $5\,\%$ of P_n. The minimum energy that needs to be reserved in the BESS for the operation of frequency regulation, during the simulation period, is closely related to the amount of charge-discharge power. The lower the recharge rate, the greater the depth of discharge of the BESS and therefore, the larger amount of minimum energy is required to be reserved.

Proportional charge-discharge strategy: This control strategy applies the notion of analog control in the state of charge of the batteries. In the previous control strategy the charging-discharging power remained constant at a predetermined power level, regardless the proximity of the battery SOC to the SOC_{ref}. In proportional control, any deviation from the specified value (SOC_{ref} in our case) is considered as an error and, therefore the larger the error, the greater the power that restores the system to its reference condition. The objective now is to regulate the battery SOC when the system is inside the non-critical window with variable charge-discharge power, which depends on how far from the SOC_{ref} the system is [13].

The operation rule of the algorithm can be formulated in relation to eq. (6) in the following way:

$$P_{VSG} = \begin{cases} K_p \cdot (f - f_{ref}) + K_d \cdot \dfrac{df}{dt}, & |\Delta f| \geq 20\,\mathrm{mHz} \\ K_{soc} \cdot \dfrac{(SOC - SOC_{ref})}{\Delta SOC_{max}}, & |\Delta f| < 20\,\mathrm{mHz} \end{cases} \tag{7}$$

where, $\Delta SOC_{max} = |SOC_{ref} - SOC_{min}| = 0.2$. The constant fraction ${}^{K_{soc}}/_{\Delta SOC_{max}}$ is calculated in such a way that a portion of charge-discharge power ($0.01P_n\ to\ 0.05P_n$) is activated when the change in the state of charge reaches the operational boundaries of the storage system. Therefore, the charge-discharge power is a portion of the normalized coefficient K_{soc} by the ratio $^{(SOC-SOC_{ref})}/_{\Delta SOC_{max}}$.

The graph in Fig. 13 show the depth of discharge of the storage as a function of time for different modes of operation with K_{SOC} of $1\,\%$, $3\,\%$, and $5\,\%$ of P_n.

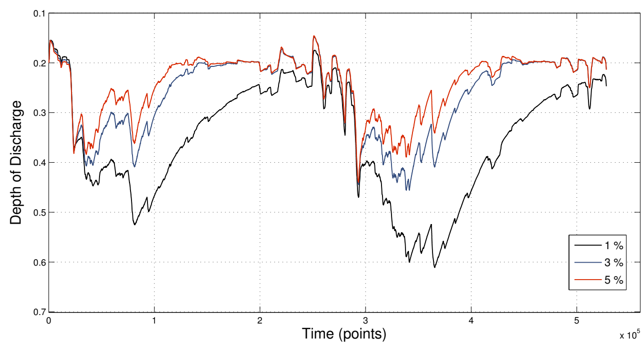

Fig. 13. Depth of discharge of the storage as a function of time for different modes of operation with K_{SOC} of $1\,\%$, $3\,\%$, and $5\,\%$ of P_n.

Fig. 14, places together the maximum depth of discharge and the maximum charge-discharge power that occurred as a function of the K_{soc} for the aforementioned control strategies. Primarily, it illustrates the effect of increasing the rate of charge-discharge power on the maximum depth of discharge of the system. The higher the coefficient K_{soc} is, and therefore the rate of charge-discharge power, the lower the maximum depth of discharge of the storage, until a threshold where further increase makes no real change. A small K_{soc} value of about $4\,\% - 5\%$ of P_n is shown to be the upper limit for the system for both battery management strategies, while a smaller value seems to be sufficient to maintain the battery SOC. From the maximum depth of discharge point of view, the constant and proportional control algorithms are comparable.

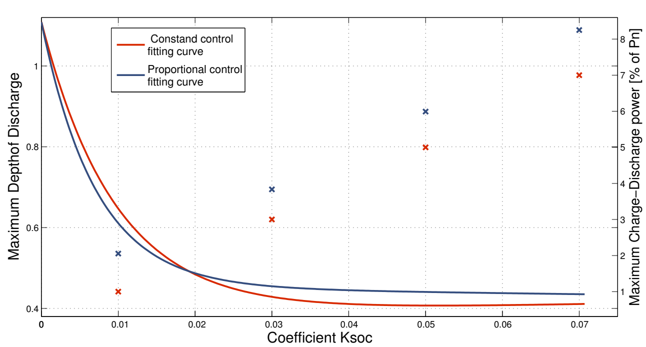

Fig. 14. Maximum depth of discharge and maximum charge-discharge power as a function of the K_{soc}.

Moreover, Fig. 14 shows the maximum charge-discharge power occurred during simulation as a function of the K_{soc}. The proportional control charges the storage system with a greater maximum power, given that this maximum power takes place only when the system exceeds the operational boundaries of the storage system (i.e. $SOC < SOC_{min}$). This happens only in few instances throughout the simulated time period when the BESS is in a critical state.

Conclusions

This paper provides a validation of the operation of the VSG in several test-networks. Simulations show that by increasing the level of penetration of the VSG, the frequency deviation induced by the load variations is improved.

A comparison of several control strategies of a battery storage system with virtual inertia support for the frequency regulation is also provided. The simulation scenarios considered herein uses real frequency data for a time period of a week. A method is adopted to evaluate the battery management strategies according to the minimum required battery capacity needed for the accomplishment of frequency regulation. The results show a good performance of both constant and proportional charge-discharge strategies. The impact of different recharge powers to the overall operation is investigated showing that a recharge power as small as $3\,\%$ of P_n is adequate for the maintenance of the *BESS*.

References

[1] M. Donnelly, J. Dagle, D. Trudnowski, and G. Rogers, “Impacts of the distributed utility on transmission system stability,” IEEE Transactions on Power Systems, vol. 11, no. 2, pp. 741 – 746, May 1996.
[2] K. Visscher and S. De Haan, “Virtual synchronous machines (VSG’S) for frequency stabilisation in future grids with a significant share of decentralized generation,” in SmartGrids for Distribution, 2008. IET-CIRED. CIRED Seminar, Jun. 2008.
[3] H.-P. Beck and R. Hesse, “Virtual synchronous machine,” in International Conference on Electrical Power Quality and Utilisation, 2007.
[4] G. W. Qing-Chang Zhong, “Synchronverters: Inverters that mimic synchronous generators,” Industrial Electronics, IEEE Transactions on, vol. 58, no. 4, pp. 1259 – 1267, 2011.
[5] T. V. Van, K. Visscher, J. Diaz, V. Karapanos, A. Woyte, M. Albu, J. Bozelie, T. Loix, and D. Federenciuc, “Virtual synchronous generator: An element of future grids,” in Innovative Smart Grid Technologies Conference Europe (ISGT Europe), 2010 IEEE PES. IEEE, Oct. 2010.
[6] J. Machowski, J. Bialek, and D. J. Bumby, Power System Dynamics: Stability and Control, 2nd ed., Dec. 2008.
[7] V. Karapanos, S. de Haan, and K. Zwetsloot, “Real time simulation of a power system with VSG hardware in the loop,” in IECON 2011 - 37th Annual Conference on IEEE Industrial Electronics Society. IEEE, Nov. 2011, pp. 3748–3754.
[8] J. F. Manwell and J. G. McGowan, “Lead acid battery storage model for hybrid energy systems,” Solar Energy, vol. 50, no. 5, pp. 399 – 405, May 1993.
[9] V. Van Thong, E. Vandenbrande, J. Soens, D. Van Dommelen, J. Driesen, and R. Belmans, “Influences of large penetration of distributed generation on n-1 safety operation,” in Power Engineering Society General Meeting, 2004. IEEE, Jun. 2004, pp. 2177 – 2181.
[10] P. M. Anderson and A. A. Fouad, Power system control and stability. Wiley, Oct. 2003.
[11] “Operational handbook: Load-frequency control and performance,” ENTSO-E, Tech. Rep. 2.5. [Online]. Available: https://www.entsoe.eu/fileadmin/user_upload/_library/publications/ce/oh/Policy1_final.pdf
[12] A. Oudalov, D. Chartouni, and C. Ohler, “Optimizing a battery energy storage system for primary frequency control,” Power Systems, IEEE Transactions on, vol. 22, no. 3, pp. 1259 – 1266, 2007.
[13] Karapanos, V., Yuan, Z., de Haan, S. W. H., and Visscher, K., “A control algorithm for the coordination of multiple virtual synchronous generator units,” in Proceedings of the IEEE Powertech conference, June 19-23, Trondheim, Norway, 2011.